

4-20-2005

Cantilever tilt compensation for variable-load atomic force microscopy

Rachel J. Canara
University of Wisconsin

Matthew J. Brukman
University of Wisconsin

Robert W. Carpick
University of Pennsylvania, carpick@seas.upenn.edu

Copyright (2005) American Institute of Physics. This article may be downloaded for personal use only. Any other use requires prior permission of the author and the American Institute of Physics. Reprinted in *Review of Scientific Instruments*, Volume 76, Issue 5, Article S3706, May 2005, 6 pages.

NOTE: At the time of publication, author Robert W. Carpick was affiliated with the University of Wisconsin. Currently (June 2007), he is a faculty member in the Department of Mechanical Engineering and Applied Mechanics at the University of Pennsylvania. Publisher URL: <http://dx.doi.org/10.1063/1.1896624>

This paper is posted at Scholarly Commons. http://repository.upenn.edu/meam_papers/90
For more information, please contact repository@pobox.upenn.edu.

Cantilever tilt compensation for variable-load atomic force microscopy

Rachel J. Cannara

Department of Physics, University of Wisconsin, Madison, Wisconsin 53706

Matthew J. Brukman and Robert W. Carpick

Department of Engineering Physics, University of Wisconsin, Madison, Wisconsin 53706

(Received 19 January 2005; accepted 21 February 2005; published online 20 April 2005)

In atomic force microscopy (AFM), typically the cantilever's long axis forms an angle with respect to the plane of the sample's surface. This has consequences for contact mode experiments because the tip end of the cantilever, which is constrained to move along the surface, displaces longitudinally when the applied load varies. As a result, the AFM tip makes contact with a different point on the surface at each load. These different positions lie along the projection of the lever's long axis onto the surface. When not constrained by static friction, the amount of tip-displacement is, to first order, proportional to the load and is shown to be substantial for typical AFM and cantilever geometries. The predictions are confirmed experimentally to within 15% or better. Thus, care should be taken when performing load-dependent contact mode experiments, such as friction versus load, elasticity versus load, or force versus displacement measurements, particularly for heterogeneous or topographically-varying samples. We present a simple method to reliably and precisely compensate for in-plane tip displacement that depends only on the range of vertical motion used to vary the load. This compensation method should be employed in any load-varying AFM experiment that requires the tip to scan the same line or to remain at the same point at each load. © 2005 American Institute of Physics. [DOI: 10.1063/1.1896624]

I. INTRODUCTION

Atomic-force microscopy (AFM) is an invaluable tool for investigating the interactions between a nanoscale probe tip and sample surface.^{1,2} In AFM, the tip is integrated near the end of a microfabricated cantilever. The tip/cantilever assembly may be scanned across the surface of a sample of interest, or displaced normal to the surface, depending on the experiment. Common applications include topography, friction, and force-displacement (FD) measurements. In dynamic AFM, information related to topographic and material contrast are gathered via noncontact (NC) or intermittent-contact (IC) modes.³ Alternately, one can use contact mode AFM to obtain topography, elasticity, and friction data. Typical contact mode experiments, such as friction versus load (FvL), elasticity versus load, and FD measurements, involve varying the applied load between the tip and sample by ramping the normal force setpoint. A piezoelectric actuator that moves either the sample platform or cantilever holder responds to this modulation by controlling the relative displacement of the sample and the fixed end of the cantilever. This displacement, in turn, alters the amount the lever is bent.

The tip displaces as a consequence of two features inherent to the experiment: (1) the relative motion between the sample and the fixed end of the lever, and (2) the 10°–25° tilt of the cantilever with respect to the sample, typical of most AFMs. Overney *et al.* discussed the effect of in-plane displacement on elastic compliance measurements and accounted for it in their experiments.⁴ In addition, Marcus *et al.* and D'Amato, *et al.* addressed other consequences of the tilt

angle in AFM in relation to phase contrast imaging in intermittent-contact AFM.^{5,6} We continue the discussion of lever tilt and address its role in contact mode imaging and nanotribology measurements with AFM. Consider a FvL experiment in which the same line is to be scanned at a series of loads. Most commercial instruments permit the user to disable piezo motion in the slow-scan direction (the x -direction in Fig. 1). Nonetheless, the tip end of the lever displaces in this direction, i.e., parallel to the lever's projection onto the sample (the x -axis). Thus, with increasing load, i.e., with decreasing separation between the fixed end of the lever and the sample surface, the tip end of the lever moves in the $+x$ -direction. Similarly, the tip retraces this path when the lever retracts from the surface. The load-dependence of the in-plane tip position relative to features on the sample surface has been ignored or underestimated in past studies. In this paper, we demonstrate that this dependence has a strong effect on the interpretation of data and the manner in which measurements should be taken. We show that this is particularly important for surfaces with nanoscale topographic, structural, or compositional variations, and when studies of nanoscale wear are of interest.

II. LOAD DEPENDENCE OF IN-PLANE TIP-SAMPLE DISPLACEMENT

A. Preliminary observations

To illustrate this effect, we begin by discussing a FvL study of the (1 $\bar{1}$ 02) surface (R -plane) of single crystal α -alumina. Experiments are carried out using the EV scanner of a Digital Instruments (DI)/Veeco MultiMode AFM with a

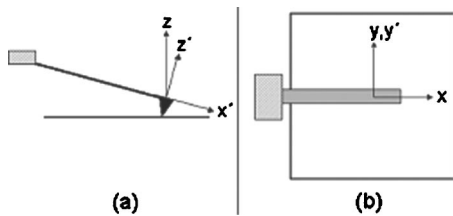


FIG. 1. (a) Side view and (b) top view of the lever-sample system in an atomic force microscope. The x -axis corresponds to the projection of the cantilever onto the sample surface. Tip-displacement (or motion of the tip end of the lever) versus load occurs along this axis. Load is varied by moving the fixed end of the lever relative to the sample along the z -axis.

Nanoscope IV controller and Signal Access Module. The EV scanner has a vertical range of approximately $2.5 \mu\text{m}$ and an x - y scan range of approximately $10 \mu\text{m}$. As shown in Fig. 1, the lever forms a nominal 11° angle between its x' - y plane and the x - y plane of the sample (which may be tilted relative to the microscope). The cantilever is held fixed while piezos drive the sample platform in x , y , and z . The $(1\bar{1}02)$ surface of our α -alumina sample is extremely flat, having a RMS roughness of 0.09 nm over a $300 \times 300 \text{ nm}^2$ region, and 0.06 nm over a $100 \times 300 \text{ nm}^2$ terrace [Fig. 2(a)].

After a series of FvL measurements (with the slow-scan disabled by the software), wear debris or swept-up particulates flank the imaged area [Fig. 2(b)]. Instead of indicating that scanning occurred on one scan line or over a narrow region, the debris forms a large rectangular pattern on the surface. It is unlikely that this wear pattern is a result of drift, as there is no evidence of similar motion in the y -direction. Moreover, the length of the x -sides of the rectangle is $160 \pm 3 \text{ nm}$, a displacement that is much larger than the thermal drift typically observed in this instrument. In this case, a load-dependent displacement between the tip and sample is the only explanation for the large size of the debris features. If the load is not varied, but scanning takes place for the same amount of time ($\sim 20 \text{ min}$), the resulting rectangle is approximately 6 nm .

The tilt effect is also apparent for tribological interfaces that exhibit atomic-scale stick-slip behavior, or for which high adhesion produces tip or lever buckling. Watson *et al.* observed atomic stick-slip behavior in the normal force signal while varying the z -displacement of an AFM cantilever relative to WTe_2 and highly oriented pyrolytic graphitic surfaces.⁷ They attribute this effect to the same mechanism

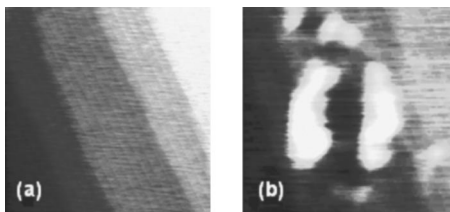


FIG. 2. $300 \times 300 \text{ nm}^2$ topographs of α -alumina before (a) and after (b) a series of FvL measurements. The vertical scales are each 10 nm . Scanning has either worn this surface or swept aside physisorbed material that now flanks the scanned region. The length of this region is a measure of the amount by which the tip displaced during the FvL experiment, where the load was ramped by 270 nN , corresponding to a z -displacement of 820 nm . The worn region extends approximately 160 nm in the x -direction.

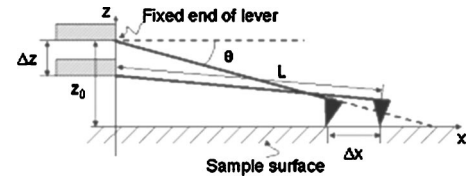


FIG. 3. Schematic of the basic geometry of a typical lever-sample system at zero and nonzero (positive) applied loads (the fixed end of the lever is higher for the zero load case) where the lever is modeled as a rigid beam. The relative position between the tip and sample changes as the applied load varies. Increased load decreases the relative separation between the base of the cantilever and the sample surface. Since the tip is constrained to the sample plane, the lever must deflect counterclockwise about its base, and the tip displaces along the $+x$ -direction.

observed here, namely longitudinal travel of the tip due to cantilever tilt. Stick-slip arises because in-plane forces are great enough to induce lever buckling.

B. Displacement versus load calculations

The extent of tip-sample displacement along the x -direction (x -displacement) depends on the lever-sample geometry specific to each AFM. Figure 3 depicts the basic geometry of the typical lever-sample system at zero and nonzero (positive) applied loads. For a given range of load, x -displacement increases with an increase in the angle θ between the cantilever and its projection onto the sample surface. The length of the cantilever and, more importantly, the range of vertical motion, Δz , also affect the total x -displacement, Δx . If we assume the lever is rigid (i.e., ignore elastic bending deformations) and that it slips without static friction, then the following simple equation describes the geometric relationship between Δx , L , θ , and Δz , as illustrated by Fig. 3,

$$\Delta x = \sqrt{L^2 - (L \sin \theta - \Delta z)^2} - L \cos \theta, \quad (1a)$$

where L is the length from the base of the lever to the tip axis, and θ is the angle between the cantilever and the sample surface at zero applied load. To first order in Δz , Eq. (1a) reduces to

$$\Delta x \approx \Delta z \tan \theta. \quad (1b)$$

The load range determines Δz , which is specific to each experiment. For an 11° tilt angle, the x -displacement is approximately 19% of the z -displacement. If the cantilever's force constant is low, then a large z -displacement is needed to vary the force appreciably. For example, to cover a load range of 100 nN using a contact mode cantilever with a force constant of 0.05 N/m requires a z -displacement of 2000 nm , thus the x -displacement is $\sim 389 \text{ nm}$.

The derivation of Eq. (1) assumes that the beam pivots rigidly about its base and does not consider elastic deformation due to bending. A second-order correction to Eq. (1a) may be obtained by considering the shape of a cantilevered, tip-loaded Euler-Bernoulli beam with uniform cross section.⁸ The result is

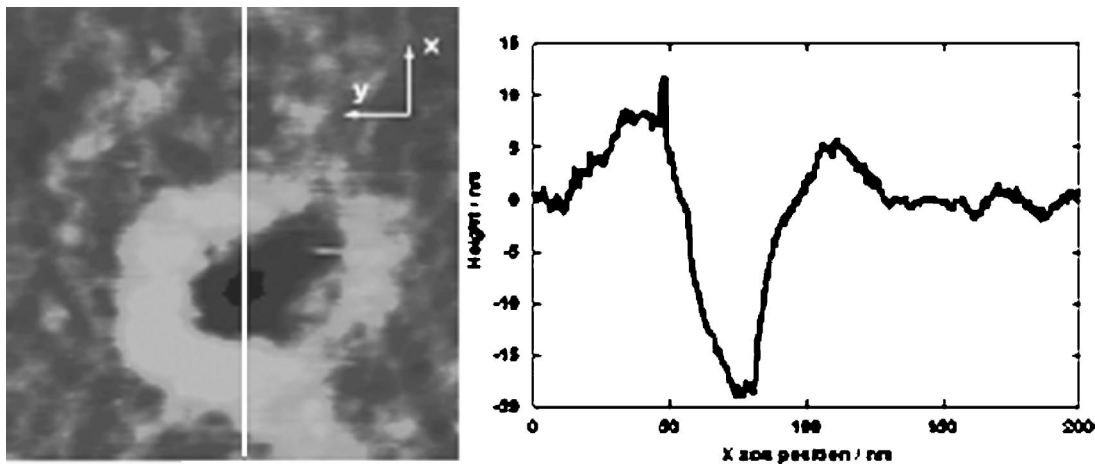


FIG. 4. AFM topograph and cross section of a wear pit in polyurethane. The top view on the left is $200 \times 200 \text{ nm}^2$ and has a height scale of 35 nm.

$$\Delta x_{\text{bending}} = -\frac{3\Delta z^2}{L} \cos \theta \quad (2)$$

and the sum of Eq. (1) and Eq. (2) give the total in-plane deflection. Equation (2) yields a 5% reduction from the rigid analysis of Eq. (1) for small bending deflections of the cantilever. For most measurements, this small correction may be neglected. Equation (1) also neglects sample drift, tip bending, and lever buckling. There may indeed be cases where it is important to address the role of each of these effects in an experiment depending on the conditions. For example, if friction is very high, the tip may not slip at first and could remain constrained to one contact point for a substantial range of loads. This effect was seen by Enachescu *et al.*⁹

C. Theory versus measurement

The dependence predicted by Eq. (1b) can produce a substantial x -displacement in an experiment. Thus, it is easy to measure the distance traversed in the ix -direction by the tip for FvL measurements that produce wear by examining the wear debris. With the range of loads used in the α -alumina experiment, $\Delta z = 816 \text{ nm}$, and the tilt angle $\theta = 11^\circ$. In this case, Eq. (1b) predicts a total x -displacement, $\Delta x = 159 \text{ nm}$. [Equation (2) would add another 8 nm to the predicted value.] From the wear debris in Fig. 2(b), we measure $\Delta x = 160 \pm 3 \text{ nm}$, in remarkable agreement with Eq. (1b).

This is an especially significant result if the goal of an experiment is to repeat measurements on the same location on the sample at different loads. Moreover, if the surface is chemically or topographically inhomogeneous, it is futile to compare data at different loads without some form of compensation.

Further direct evidence of tip displacement was obtained by performing load variation experiments on polyurethane and on a monolayer-coated alumina single crystal sample. The normal force setpoint was ramped over substantial load ranges (the maximum was approximately 130 nN) several times according to a sawtooth waveform with the fast scan on and the slow scan off. Resulting wear pits in the material were observed in topographic images (Fig. 4). Three cantilevers of different lengths and force constants were used. The results, included in Table I along with other measurements discussed in this section, show excellent agreement with the predictions of Eq. (1b), with measured values generally being less than predicted, but within the substantial uncertainties of determining the boundaries of the wear pits. In particular, the low-load region of the wear pit is shallowly sloped, making it somewhat difficult to distinguish it from the surrounding unworn region. Moreover, polyurethane is a viscoelastic material, and some relaxation of the surface is expected after unloading, thereby altering the shape of the wear pit. The force threshold for permanently deforming the

TABLE I. Summary of predicted and measured x -displacements from wear experiments on a polyurethane, a PA SAM film, and α -alumina.

Surface	Lever type	Length / (μm)	Δz / (nm)	Δx predicted to 1st order / (nm)	Δx predicted to 2nd order / (nm)	Δx Measured / (nm)	% Agreement with 1st order prediction
Polyurethane	SN	100	263	51	51	45 ± 5	88 ± 10
Polyurethane	SN	100	263	51	51	58 ± 8	114 ± 16
Polyurethane	Si	110	304	59	58	50 ± 10	85 ± 17
Polyurethane	SN	200	397	77	77	77 ± 10	100 ± 13
Polyurethane	SN	200	397	77	77	65 ± 15	84 ± 19
PA SAM	SN	200	493	96	95	92 ± 10	96 ± 10
α -Alumina	Si	300	81	159	158	160 ± 3	101 ± 2

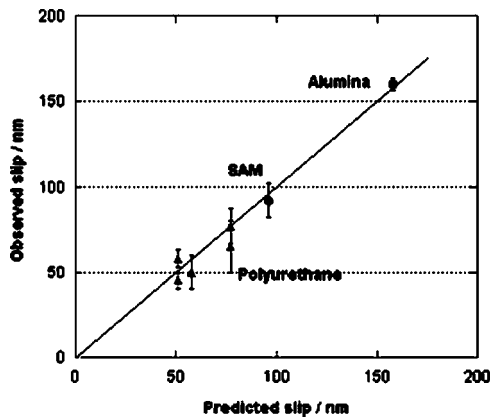


FIG. 5. Comparison of predicted and observed tip slip. The 45° line represents theoretical perfect agreement.

polyurethane is unknown, but any nonzero value would result in a systematic reduction in the observed x -displacement, as it would occur at low loads, but without corresponding wear.

A similar test was performed on a monolayer-coated α -alumina sample. A phosphonic acid self-assembled monolayer (PA SAM) was seen to have loosely-bound material on the surface that could be pushed with the AFM tip at small positive loads, but was undisturbed by zero-load topographic imaging. Over the course of several load-variation cycles, the tip cleared a region of the loosely bound material, and dimensions of that region confirmed the amount of x -displacement in agreement with Eq. (1b), also shown in Table I.

The data in Table I are presented in a graphical format in Fig. 5. The scatter plot shows the predicted versus measured x -displacement and a solid line with slope=1, representing theoretical agreement between the two. The points fall very close to this line, which illustrates the good agreement between the measured and predicted values. Thus, in several cases we consistently find that the first order approximation in Eq. (1b) agrees to within 15% of measured values.

III. COMPENSATION FOR IN-PLANE TIP-SAMPLE DISPLACEMENT

Many AFM controllers allow the user to access various channels for monitoring output signals or to input external signals for custom operation. For example, FvL experiments often require an external voltage source to ramp the normal force or deflection setpoint. Similarly, proper external control of the x -piezo voltage can compensate for unwanted tip-displacement during load-dependent measurements. In a varying load experiment, the x -piezo may be ramped in the $\pm x$ -direction and in phase with the load ramp (depending upon whether the x -piezo moves the base of the lever or the sample platform) to counteract tip motion in the $+x$ -direction. The experiments below demonstrate the effectiveness of this external slow-scan control.¹⁰

FvL measurements are performed with SN and tungsten carbide-coated (WC) tips on the (111) surface of hydrogen-terminated single-crystal diamond. Cantilever dimensions are measured optically or by TEM, and their relevant values

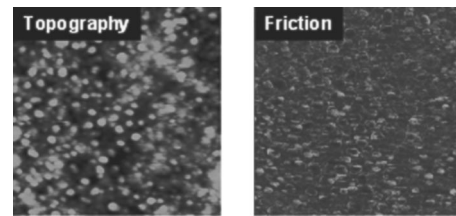


FIG. 6. $500 \times 500 \text{ nm}^2$ AFM topography and friction images of the H-terminated diamond (111) surface, using a 13.5 nm radius tungsten carbide-coated Si tip. The RMS roughness at this scale is 1–3 nm, and the surface consists of islands with a $\sim 0.3 \text{ nm}$ RMS roughness.

are given in Table I, along with the data for each cantilever used in this work. Normal spring constants and lateral forces are calibrated according to established methods.^{11,12} Van den Oetelaar *et al.* showed that H-termination reduces atomic-scale friction on diamond in an ultrahigh vacuum environment.¹³ Although the present work is conducted in air ($\text{RH} \cong 60\%$), an H-terminated surface is employed to help minimize friction and adhesion. Therefore, prior to FvL measurements, the diamond sample is cleaned in an acid bath and H-terminated in a H_2 plasma.^{14,15} This procedure produces a chemically inert, C–H bonded surface with a water contact angle of 85° – 87° .

Figure 6(a) shows a $500 \times 500 \text{ nm}^2$ AFM topograph of the diamond C(111)–H surface. The image has a RMS roughness of 1–3 nm and consists of 20–50 nm islands of approximately 0.3 nm rms roughness, consistent with previous work.^{13,16} The islands are regions of relatively low friction surrounded by stepped features of higher friction [Fig. 6(b)]. As a result, FvL measurements (without x -compensation) produce abnormal data in which friction increases nonmonotonically with load (Fig. 7). If not aware of the x -displacement effect, one might suspect that tip wear was responsible for the nonmonotonic variations in friction. However, the abnormal data were often highly repeatable multiple times, for both increasing and decreasing loads, which would not be expected for irreversible tip wear processes. Figure 8 shows FvL measurements taken with a WC tip at two different locations on the sample, alternating back and forth between them. No other scanning occurs between

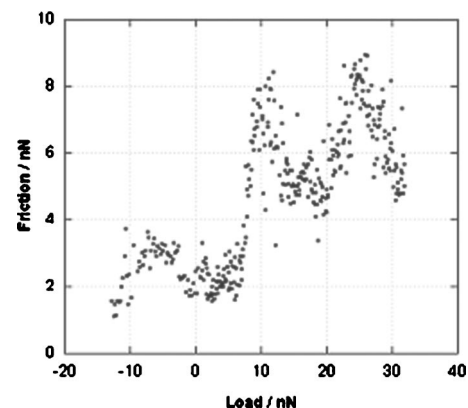


FIG. 7. Friction on the H-terminated diamond sample without x -displacement compensation results in abnormal behavior. Friction varies nonmonotonically with load as a result of either topographical or chemical inhomogeneities on the surface.

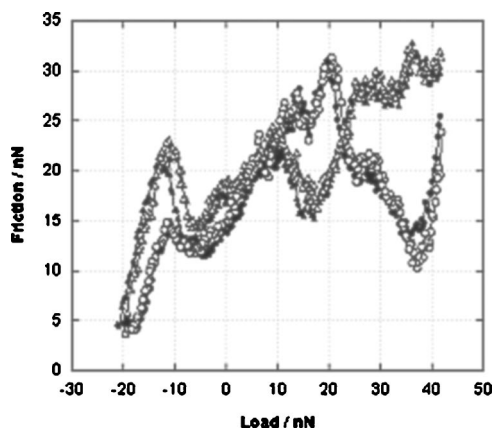


FIG. 8. The positions of two islands, A and B, were identified and friction versus load measurements taken alternating between those two positions (starting with A) without additional scanning between each measurement. Circles and triangles correspond to islands A and B, respectively. The data plotted with open symbols were acquired after the data plotted with the closed symbols. The nonmonotonic friction behavior is reproducible at each location. For clarity, the data shown here correspond to decreasing load only.

data acquisition at each position. Each location exhibits its own reproducible nonmonotonic variations. This rules out tip wear as the explanation for the variations in friction, and it suggests that nonmonotonic friction is instead an artifact of surface inhomogeneities (topographical and/or chemical). Furthermore, we obtain TEM images of the tip before and after the experiment and observe little to no tip wear. Although tip wear takes place in some cases, it does not occur with every measurement. In contrast, the abnormal friction behavior shown in Figs. 8 and 9 is observed without exception when no x -compensation is used.

Figure 9 compares FvL data for a SN tip on the same 30 nm island of C(111)-H with and without x -compensation. In this case, $\Delta z = 0.705 \mu\text{m}$, and, therefore, $\Delta x = 136 \text{ nm}$. By multiplying Δx by the x -piezo sensitivity (0.047 V/nm), we obtain the x -piezo voltage necessary to compensate for this motion (in this case, 6.39 V). This range of voltage was ap-

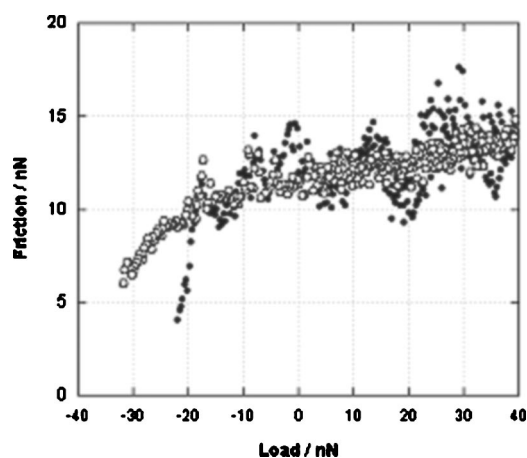


FIG. 9. Comparison between two friction versus load measurements taken with a SN tip on the same C-H island, at the same nominal position, but with x -compensation enabled (open circles) then disabled (closed circles). The nonmonotonic behavior is absent when x -compensation is used, due to the elimination of unwanted x -displacement across topographic and/or chemical variations on the surface.

plied to the piezo to cause displacement in the x -direction concurrently and in phase with the load variation. The friction data from these x -compensation measurements (open circles in Fig. 9) now increase monotonically with load. The tip has remained on or near the same line at each load. At worst, x -compensation confines the tip to within the same 30 nm island.¹⁷ Therefore, x -compensation of the piezo motion, by an amount predicted by Eq. (1), successfully preserves the tip's position on the sample as the load is varied.

IV. DISCUSSION

Longitudinal (x -) displacement of the tip with respect to the sample is significant in load-varying AFM experiments due to the tilt of the cantilever. Nonetheless, this tilt effect can be corrected precisely via x -compensation, provided that static friction is not so high as to prevent slippage of the tip appreciably. This technique is crucial to a variety of nanotribological and nanomechanical research studies, such as studies of wear in which it is important to scan the same line over a range of loads,¹⁸ chemical force microscopy (CFM) when tip-sample separation must be restricted to the direction normal to the surface for adhesion measurements on spatially or chemically heterogeneous surfaces,^{19,20} and carbon nanotube buckling experiments for which pure axial loads are desired. Most previous work has neglected this effect, despite its importance for experiments that employ long contact mode levers with low force constants. Even NC or IC mode cantilevers, if they are used for contact mode experiments, such as buckling or CFM measurements, exhibit significant x -displacements. Therefore, users should be aware of this effect and account for it when possible.

ACKNOWLEDGMENTS

The authors would like to thank Suresh Vagarali at General Electric Superabrasives for graciously supplying the diamond sample used in this work; Matthew J. D'Amato for preparing and providing the polyurethane sample; Timothy D. Dunbar of 3M Company for providing the PA SAM crystal; UW-Madison Professor Robert J. Hamers' group for help with and use of their hydrogen plasma chamber; and the National Science Foundation CAREER Award for funding this work.

¹G. Binnig, C. F. Quate, and C. H. Gerber, *Phys. Rev. Lett.* **56**, 930 (1986).

²C. M. Mate, G. M. McClelland, R. Erlandsson, and S. Chiang, *Phys. Rev. Lett.* **59**, 1942 (1987).

³R. García and R. Pérez, *Surf. Sci. Rep.* **47**, 197 (2002).

⁴R. M. Overney, H. Takano, and M. Fujihira, *Europhys. Lett.* **26**, 443 (1994).

⁵M. S. Marcus, R. W. Carpick, D. Y. Sasaki, and M. A. Eriksson, *Phys. Rev. Lett.* **88**, 226103 (2002).

⁶M. J. D'Amato, M. S. Marcus, M. A. Eriksson, and R. W. Carpick, *Appl. Phys. Lett.* **85**, 4738 (2004).

⁷G. S. Watson, B. P. Dinte, J. A. Blach-Watson, and S. Myhra, *Appl. Surf. Sci.* **235**, 38 (2004).

⁸R. D. Cook and W. C. Young, *Advanced Mechanics of Materials*, 2nd ed. (Prentice-Hall, Upper Saddle River 1999).

⁹M. Enachescu, R. W. Carpick, D. F. Ogletree, and M. Salmeron, *J. Appl. Phys.* **95**, 7694 (2004).

¹⁰For a homogenous surface, x -compensation may be achieved by enabling the slow-scan motion in the imaging software and by selecting a scan size equal to Δx . For inhomogeneous samples, it is necessary to choose a

y -scan length that is smaller than Δx , but AFM software rarely permits aspect ratios for which the x -scan size is larger than y . In this situation, we use a function generator as the voltage source for x -compensation.

- ¹¹J. E. Sader, *Rev. Sci. Instrum.* **70**, 3967 (1999).
- ¹²D. F. Ogletree, R. W. Carpick, and M. Salmeron, *Rev. Sci. Instrum.* **67**, 3298 (1996).
- ¹³R. J. A. v. d. Oetelaar and C. F. J. Flipse, *Surf. Sci.* **384**, L828 (1997).
- ¹⁴B. D. Thoms, M. S. Owens, J. E. Butler, and C. Spiro, *Appl. Phys. Lett.* **65**, 2957 (1994).
- ¹⁵W. Yang, O. Auciello, J. E. Butler, W. Cai, J. A. Carlisle, J. E. Gerbi, D. M. Gruen, T. Knickerbocker, T. L. Lasseter, J. John N. Russell, L. M. Smith, and R. J. Hamers, *Nat. Mater.* **1**, 253 (2002).
- ¹⁶M. Enachescu, R. J. A. v. d. Oetelaar, R. W. Carpick, D. F. Ogletree, C. F. J. Flipse, and M. Salmeron, *Phys. Rev. Lett.* **81**, 1877 (1998).
- ¹⁷These x -compensation tests are successful, in part, because there is little drift during each measurement. In general, drift will render x -compensation useless, unless some additional compensation is employed to account for drift.
- ¹⁸J. D. Batteas, X. Quan, and M. K. Weldon, *Tribol. Lett.* **7**, 121 (1999).
- ¹⁹D. V. Vezenov, A. Noy, and P. Ashby (to be published).
- ²⁰In CFM and FD, x -compensation should be used only in the repulsive regime, when the tip is geometrically constrained to the surface. It is therefore a difficult exercise to ensure that the tip remains above the same point on the surface throughout the measurement.